○ **Micro and Nano Systems Letters**

Methods to analyze extracellular vesicles at single particle level

Yongmin Kwon[1] and Jaesung Park[1,2]* ○iD

Abstract

Extracellular vesicles (EVs) are nano-sized vesicles derived from cells that transport biomaterials between cells through biofluids. Due to their biological role and components, they are considered as potential drug carriers and for diagnostic applications. Today's advanced nanotechnology enables single-particle-level analysis that was difficult in the past due to its small size below the diffraction limit. Single EV analysis reveals the heterogeneity of EVs, which could not be discovered by various ensemble analysis methods. Understanding the characteristics of single EVs enables more advanced pathological and biological researches. This review focuses on the advanced techniques employed for EV analysis at the single particle level and describes the principles of each technique.

Keywords: Extracellular vesicle, Single particle analysis, Nanoparticle tracking analysis, Nano-flow cytometry, Total internal reflection fluorescence microscopy, Dark-field microscopy, Electron microscopy, Atomic force microscopy, Resistive pulse sensing

Introduction

Extracellular vesicles (EVs) are nano-sized vesicles derived from cells that transport biomaterials between cells through biofluids [1]. Since EVs were discovered as part of Hodgkin's disease research in 1978, their biological roles and potential for drug delivery and clinical diagnosis have been attracting attention [2–5]. EVs are composed of a phospholipids, cholesterol, fatty acids, and membrane proteins. They contain genetic information such as RNAs and DNAs inside, acting as biological carriers related to cell division and productivity (Fig. 1a). Owing to these biological properties, they have been considered as potential drug carriers and for diagnostic applications [2, 3, 6, 7]. EVs are classified into exosomes (50–200 nm), microvesicles (200–1000 nm), and apoptotic bodies (1–5 μm according to their size and cellular origin (multivesicular bodies, plasma membrane driven, apoptotic cell) (Fig. 1b). Various methods are employed to isolate EVs from culture media to study their relevance to biological roles. There are several isolation methods, including density difference (ultracentrifugation, density gradient ultracentrifugation), size-based isolation (size exclusion chromatography, membrane filter), and chemical affinity-based isolation (immunoaffinity, polymer-based precipitation) [8, 9]. EVs obtained from various types of cells and isolation methods are essential for characterization and identification for research and biological applications. Although there are no specifically proposed specific markers for identifying EVs, they can be analyzed using their membrane protein markers including CD9, CD63, CD81, TSG101, and Alix [10].

Biological analyzes such as western blots, polymerase chain reaction (PCR), and dynamic light scattering (DLS) provide a tendency to have significantly different components depending on the cell line and isolation method. However, only their biological and physical representativeness has been analyzed through ensemble analysis of EV groups and such analysis is insufficient to identify the biophysical and biochemical characteristics of EVs and their roles. The development of analysis techniques has made it possible to employ analysis at the single particle

*Correspondence: jpark@postech.ac.kr
[1] Department of Mechanical Engineering, Pohang University of Science and Technology (POSTECH), Pohang, Gyeong-buk 37673, Republic of Korea
Full list of author information is available at the end of the article
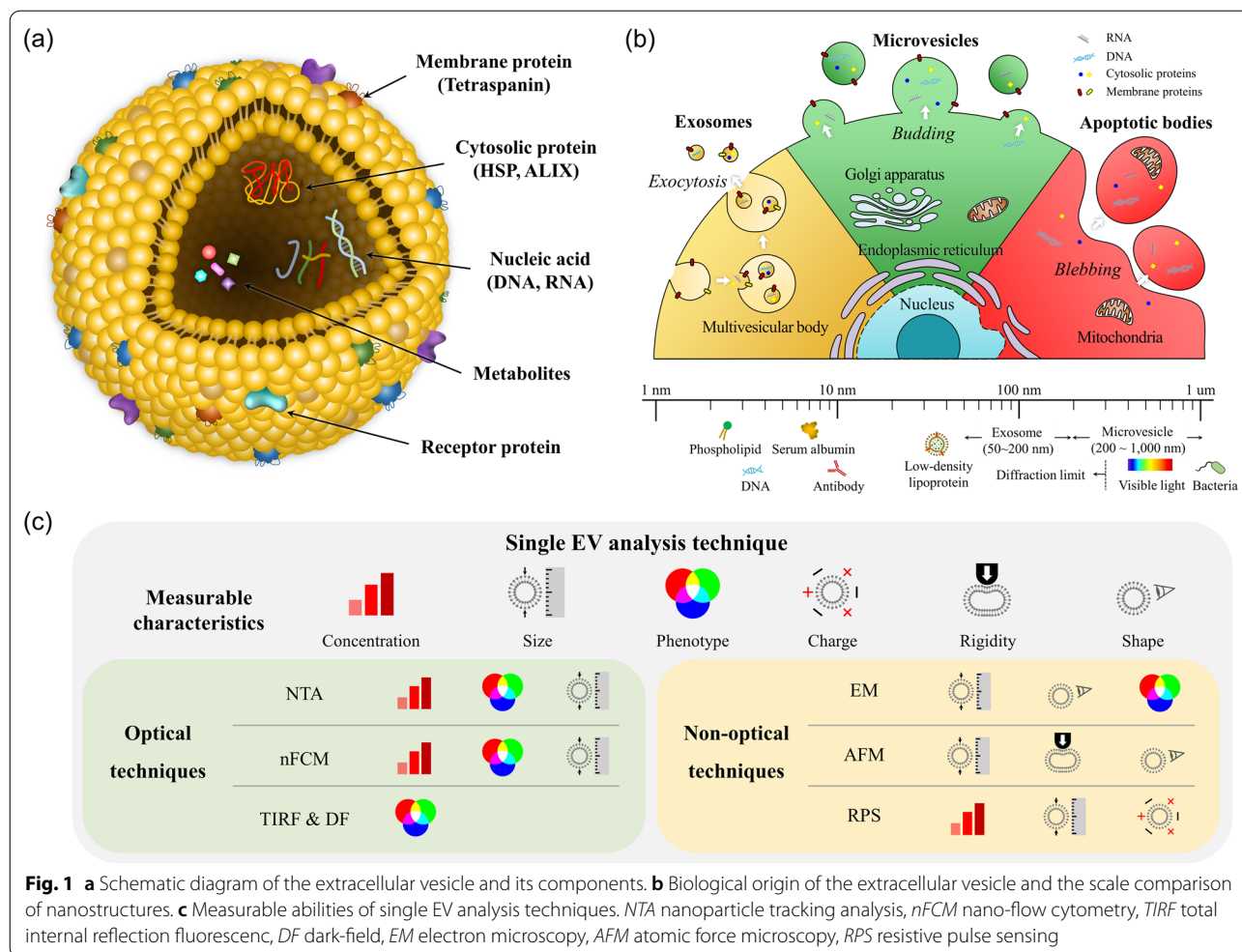
Fig. 1 a Schematic diagram of the extracellular vesicle and its components. **b** Biological origin of the extracellular vesicle and the scale comparison of nanostructures. **c** Measurable abilities of single EV analysis techniques. *NTA* nanoparticle tracking analysis, *nFCM* nano-flow cytometry, *TIRF* total internal reflection fluorescenc, *DF* dark-field, *EM* electron microscopy, *AFM* atomic force microscopy, *RPS* resistive pulse sensing

level, rather than ensemble, to identify the roles of EVs [11–13]. Single EV analysis techniques have been developed by solving challenging problems, such as the EV nanoscale size, biochemical complexes, heterogeneity of EVs, and measurement accuracy. Most developed single EV analysis techniques are aimed at analyzing physical and biochemical properties of EVs at the single particle level. The technologies developed to efficiently analyze single EVs can be mainly divided into optical and non-optical techniques (Fig. 1c).

Optical analysis represents the technique of acquiring information using light. However, EVs are difficult to directly observe with a conventional optical microscopy due to their small size that is similar to the diffraction limit. Therefore, physical information is obtained by analyzing the scattered light signal at the sub-wavelength scale, using nanoparticle tracking analysis (NTA) that tracks the scattered light signal of the diffusion of particles and flow cytometry (FCM) that uses the scattered light pattern of the single particle. In addition,

fluorescence technology uses the interaction of light and molecules to label and observe a target marker conjugated with a fluorophore. Using fluorescence, information such as the size and location of EVs can be obtained through the selective signal of single EVs with sizes below the diffraction limit. Non-optical techniques do not directly detect photons in signal measurements. Electron microscopy (EM) techniques detect scattered or transmitted electrons, and resistive pulse sensing (RPS) techniques measure changes in electrical resistance caused by EVs passing through pores. Atomic force microscopy (AFM) techniques detect the deformation of tip and measure the mechanical properties and shape of membranes. Through these various nanotechnologies, the heterogeneous characteristics and biological functions of single EVs can be analyzed and cross-validated [10]. This review describes an overall single EV analysis technique at the sub-diffraction limit scale.

Optical techniques

One of the most direct approaches to obtain information of EVs is to observe them directly. In general, optical microscopy detects objects using wavelengths in the visible light range. Unfortunately, due to the diffraction limit of visible light discovered by Ernst Abbe in 1873, EVs on the sub-wavelength scale have limitations in terms of their direct observation through optical microscopy [14].

$$d = \frac{\lambda}{2NA} = \frac{\lambda}{2n \cdot sin\theta} \tag{1}$$

In the above equation, d denotes the Abbe diffraction limit, indicating the minimum resolution to distinguish between two points. Numerical aperture (NA) is equal to the sine value of the refractive index n multiplied by the incident angle θ. The fundamental goal of single EV analysis is to find out their information through selective or limited signals of a single particle within the sub-diffraction limit range.

$$I \propto \frac{d^6}{\lambda^4}\left(\frac{n^2-1}{n^2+2}\right)^2 \tag{2}$$

In Rayleigh scattering, the intensity I is proportional to the sixth power of the particle diameter d and inversely proportional to the fourth power of the wavelength λ (n is the refractive index ratio of the EV and medium). Scattered light-based imaging can detect particles larger than about 50 nm, and scattered light from particles smaller than EVs, such as proteins and antibodies, is difficult to detect [15].

FCM, a signal-based analysis technique, uses a photomultiplier tube (PMT) or optical fibers from various angles to detect the photons emitted or scattered from a single particle. Image-based single particle analysis including NTA and several other microscopy techniques analyze information according to the optical signal intensity and position information emitted by the particle. Single EVs are analyzed with scattered light without a specific label or labeled with proteins, genes, and membrane dyes such as DiI or DiO conjugated fluorophores. The optical signal emitted by a single particle is expressed in the shape of a point spread function (PSF). Among various algorithms, the most common method involves fitting the Gaussian distribution to a single emitter signal represented by the PSF [16]. The position of the single particle is approximated through the coordinates of the fitted Gaussian distribution to determine the location of the particle [17, 18]. These data processes are an essential part of the optical analysis of single particles [19].

Nanoparticle tracking analysis (NTA)

NTA is a versatile technique capable of analyzing the concentration, size, and subpopulations of biomarkers through selective fluorescence labeling. Similarly to DLS, NTA estimates the size of EVs through their Brownian motion while floating in the medium. However, the two techniques differ in terms of their approach to the analysis. NTA is a bottom-up approach that tracks the diffusivity of single particles and generalizes individual particle data to entire groups, whereas DLS is a top-down ensemble analysis method that observes fluctuation signals of whole particles and analyzes autocorrelation functions.
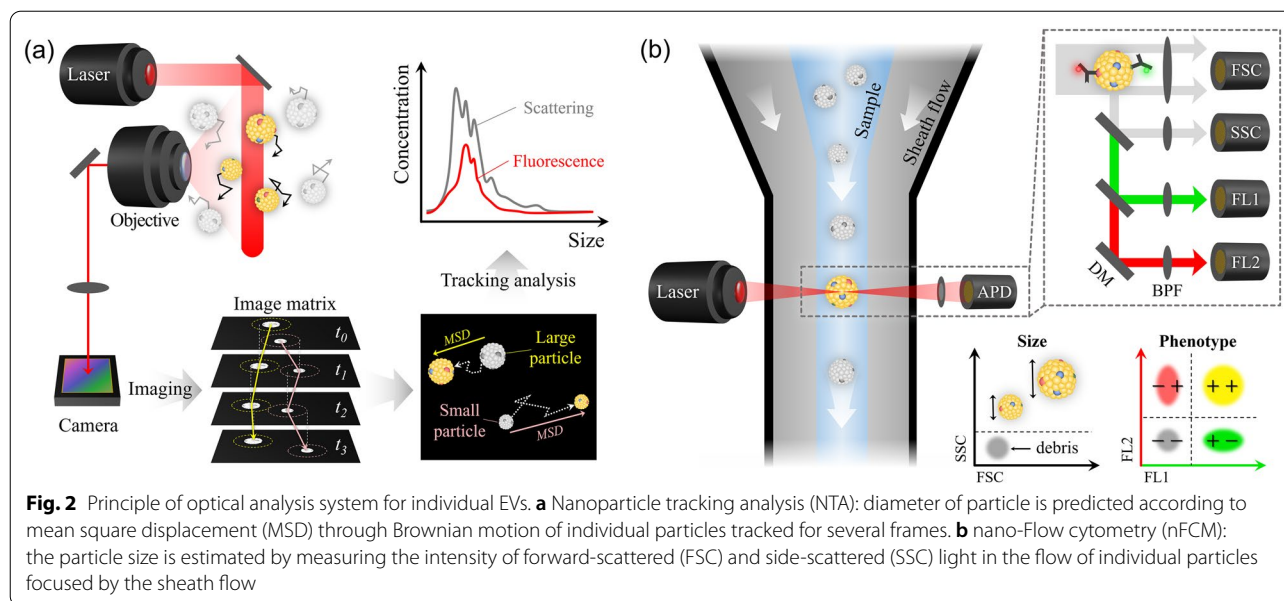
In NTA, the scattered signal of single particles is detected according to the time interval of each frame, and the signals are subsequently linked through the nearest neighborhood algorithm [20]. The Brownian motion of particles is calculated by mean squared displacement (MSD), and the diameter of single EVs is estimated from the Stokes–Einstein equation (Fig. 2a).

$$D = \frac{K_B T}{f} = \frac{K_B T}{3\pi \eta d} \tag{3}$$

$$MSD = \overline{\langle x,y \rangle^2} = \frac{4K_B T t}{3\pi \eta d} \tag{4}$$

where D is the diffusion coefficient of the spherical particle, K_B is Boltzmann's constant, and T is the thermodynamic temperature. In Stokes' law, f is the drag coefficient applied to a spherical particle with a diameter of d in a medium of viscosity η [21–24].

The tracking analysis of dynamic single EVs is dependent on the acquired images. Therefore, the most important factor to enhance the tracking accuracy is to obtain a clear particle signal with a high signal-to-noise ratio (SNR). The scatters light of EV in the Rayleigh scattering region, and the intensity is proportional to the sixth power of the diameter [15]. The measured particle size for NTA ranges from 50 nm to 1 μm. For accurate imaging and analysis, it is necessary to be prepared in a relatively uniform and appropriate size so as to avoid interference by other signals due to the exceptionally strong scattered light of large or aggregated particles. Furthermore, samples with excessively high concentrations cause detected particles to misconnect with other particle signals around them and pose challenges for tracking analysis that requires linking particles over multiple frames [7, 25]. To obtain a high SNR, commercial NTA technology uses highly inclined thin illumination (HILO) for the incident beam to minimize the difference between the laser thickness and depth of focus (DOF) and reduce out-of-focus noise [15, 26].

Fig. 2 Principle of optical analysis system for individual EVs. **a** Nanoparticle tracking analysis (NTA): diameter of particle is predicted according to mean square displacement (MSD) through Brownian motion of individual particles tracked for several frames. **b** nano-Flow cytometry (nFCM): the particle size is estimated by measuring the intensity of forward-scattered (FSC) and side-scattered (SSC) light in the flow of individual particles focused by the sheath flow

When only relying on the scattered light signal, it is impossible to distinguish between EVs and other nanoparticles of similar size, such as nanobubbles and protein aggregates. To this end, NTA combined with a fluorescent labeling method is being developed. A fluorescence-NTA (fl-NTA) technique was reported to label EVs with membrane-labeling dyes, containing DiO, DiI, and PKH dyes to specifically discriminate vesicles composed of phospholipids [18, 26, 27]. Furthermore, it is possible to quantitatively analyze specific target EV markers, such as proteins or nucleic acids conjugated with various fluorophores [Alexa Fluor, CF dye, quantum dot (Qdot), etc.] [18, 27–30]. Dragovic et al. isolated the syncytiotrophoblast exosome and microvesicle from placental-derived syncytiotrophoblast EVs and analyzed EVs stained with a Qdot-conjugated anti-PLAP antibody through fl-NTA. Each population was reported to be effectively separated. Recently, Cho et al. introduced a multi-fl-NTA with time-sequential illumination by different wavelengths that allows simultaneous analysis of the subpopulations of three proteins by fluorescence labeling of specific protein markers such as CD9, CD63, and CD81 [31]. Fluorescent labeling is a useful tool that distinguish EVs from other particles and impurities. However, lipophilic dyes for staining EVs can form micelles or aggregates due to their structural properties. Because these particles are difficult to physically distinguish from EVs, the pure dye signal must be checked before labeling EVs [28, 32, 33].

Nano-flow cytometry (nFCM)

FCM is a single particle analysis technique that measures particles aligned in a center stream by a sheath flow within a micro-channel (Fig. 2b). Single particle analysis is possible through the measurement of fluorescence signals and scattered light signals in two directions, namely, forward-scattered light (FSC) and side-scattered light (SSC) (Fig. 2b) [34]. Conventional FCM is a useful technique for measuring the size, concentration, and phenotype of particles of several microns with high accuracy and reproducibility. However, it has limited application to nanoscaled EVs. nFCM solved the limitations of nanoscale analysis of conventional FCM through technical optimization [35–37].

Quantitative and qualitative analysis of nano-sized EVs is possible using high-resolution flow cytometry by a high-performance PMT, low pressure, and optimized sheath flow [38]. The reduced flow rate achieved by the low sheath rate increases the exposure time of EVs and enables precise signal detection and measurements of particles of about 50 nm diameter [35, 38, 39]. Furthermore, to detect the FSC and SSC of sub-diffraction limit scaled particles, the angular difference between the two detectors of about 15° to 150° is required (whereas a typical FCM spans from 0.5° to 15°) [36, 40, 41].

When high concentrations of particles are suspended in the sheath fluid, the signals of single particles are overlapped, creating a swarm effect and causing coincidental detection. The concentration of particles to ensure the accuracy of quantification analysis must be

about 10^7 to 10^9 particles 1 ml [42]. When scattered light and fluorescence signals of single EVs are constant in a dilution of an appropriate concentration, accurate marker identification and sub-population analysis are possible [43, 44]. A laboratory-built high-sensitivity flow cytometer (HSFCM) manufactured by the Xiaomei Yan group enabled particle analysis of several nanometers through the optimization of laser power and dwell time [39]. Similarly to NTA, fluorescence labeling enables the distinction between EVs and impurities in nFCM. By labeling phosphatidylserine-exposing EVs with fluorescent annexin V, a more specific EV population is detected than by using only scatter signals [45]. Using HSFCM, Tian et al. stained EVs expressing CD9, CD63, and CD81 and compared the sub-population of the two markers at the same time. Furthermore, in one study, CD147, a colorectal cancer marker, was fluorescently stained to compare the difference in the expression rates between the patient group and healthy donors in EVs [35]. Morales-Kastresana et al. analyzed lipid, protein, and RNA-based EV staining methods using nFCM and found that amphiphilic dyes or SYTO RNASelect formed micelles or aggregated dyes even in the absence of EV [43]. This suggests that, as ment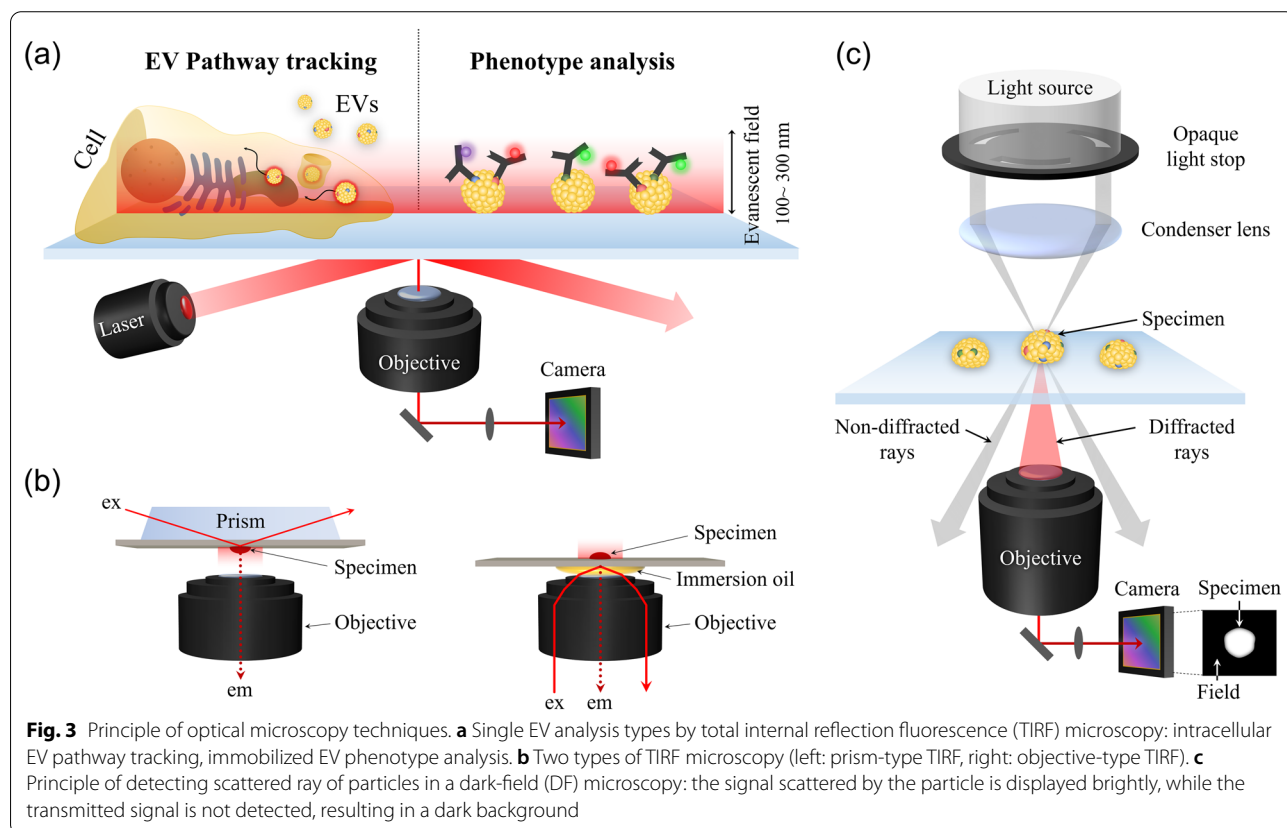ioned above, it is necessary to measure the aggregation of dyes in the fluorescent labeling or the background signal of the base buffer as a control before performing the EV analysis using labeling.

Total internal reflection fluorescence (TIRF) microscopy and dark-field (DF) microscopy

TIRF microscopy is an optical technology that enables high resolution and intuitive analysis of the biological complexity of single EVs without additional data analysis [46]. The thin evanescent field region penetrated during total internal reflection enables EV analysis near the surface. In the evanescent field, the transmitted energy decays exponentially with the distance from the surface. When it is about 1/e compared to the initial transmitted intensity, the depth is referred to as the penetration depth.

$$d = \frac{\lambda}{4\pi \sqrt{n_1 \cdot sin^2\theta - n_2}} \tag{5}$$

In the above equation, d is the penetration depth, λ is the wavelength of the incident light, and θ is the incident angle. n_1 and n_2 are the refractive indices of glass and medium. Generally, the penetration depth is about 100–300 nm. Therefore, only selectively excited fluorescently

Fig. 3 Principle of optical microscopy techniques. **a** Single EV analysis types by total internal reflection fluorescence (TIRF) microscopy: intracellular EV pathway tracking, immobilized EV phenotype analysis. **b** Two types of TIRF microscopy (left: prism-type TIRF, right: objective-type TIRF). **c** Principle of detecting scattered ray of particles in a dark-field (DF) microscopy: the signal scattered by the particle is displayed brightly, while the transmitted signal is not detected, resulting in a dark background

labeled EVs are detected, which enables high SNR imaging. Thus, the light sheet does not excite out-of-focus signal and hence reduces the background noise (Fig. 3a). Furthermore, TIRF microscopy does less photodamage to the sample than the epi-fluorescence microscopy.

TIRF microscopy is typically categorized into two types: the prism type and objective type (Fig. 3b). In the prism type, the light source is incident through the prism, the scattering noise is low, and the scalability of the sample type and position are high. In the objective type, an objective lens with a high NA is used, and the sample must be located within the focus area. High-NA objectives can acquire high-resolution images through near-field imaging [47].

Although the illuminated area of TIRF microscopy is the thinnest light sheet achievable with existing optical techniques, it is limited to analysis only near the surface. Therefore, the nanoparticles in suspension are either immobilized, or their behavior is restricted through micro-channels on the surface. Imaging of surface-immobilized EVs is the conventional method to analyze single EVs [48, 49]. Han et al. immobilized single EVs to a dimethyldichlorosilane modified glass surface using avidin–biotin complex and analyzed the sub-population of membrane proteins according to the method of EV separation [48]. A method for indirectly measuring the size of fluorescently labeled liposomes immobilized on the bottom of a coverslip with an avidin–biotin complex was likewise reported [50]. However, cell-derived vesicles are composed of heterogeneous membrane components, and there may be errors in estimating the size of the EVs from the fluorescence signal by staining only specific components such as lipids, proteins [32, 33].

In the evanescent field region, only the signal of a monolayer in the membrane and an organelle in contact with the substrate of a living cell can be observed. Pathway analysis of single EVs interacts with intracellular organelles, or the cell membrane is traced by detecting labeled EVs [51, 52]. Because the total internal reflection is sensitive to the refractive index of the medium, attention must be paid to the complex and heterogeneous refractive index of the intercellular environment [53, 54]. Hoshino et al. revealed the relationship between EVs and cell invadopodia through localization of the invadopodia actin and EV markers, such as CD63 and Rab27a [55].

He et al. analyzed exosomes fluorescently labeled by Mg^{2+}-dependent DNAzyme, using microfluidic channels. They quantified miRNAs via fluorescence intensity at the single particle level [56]. In addition, methods using TIRF microscopy for the analysis of sub-populations of single EVs flowing along micro-channels are currently being developed [57].

DF microscopy detects scattered light diffracted by the specimen Non-diffracted rays that pass directly beyond the background cannot pass through the lens and their signal is lost and darkened. Meanwhile, the diffracted rays scattered by the object pass through the lens and their signal is acquired as a bright image (Fig. 3c). DF microscopy for measuring the Rayleigh scattering of nano-sized metal particles has been studied and applied to single EV analysis in combination with various optical techniques [58–61]. The advantage of DF microscopy is that it can optically observe EVs without labeling them [60].

Generally, DF microscopy is combined with TIRF to acquire the scattered signal with a resolution of 30 to 40 nm [62]. Scattered signals are imaged using prism- or objective-type TIRF with a perforated mirror [63]. Akagi et al. used laser illumination dark-field microscopy and on-chip microcapillary electrophoresis to measure the zeta-potential of single EVs [64]. They measured the scattered light signals of single EVs and the migration of particles to confirm the relationship between the zeta-potential and desialylation of prostate cancer cell-derived EVs without labeling. The authors reported that cancer cell-derived EVs contain more sialic acid and a larger negative charge [64].

Non-optical techniques
Electron microscopy (EM)

EM is the representative technique for solving the optical diffraction limit of EV analysis. The accelerated electron beam is scattered on or transmitted through the specimens, and imaging is possible with a resolution of several nanometers. By calculating the relationship between the acceleration voltage and the wavelength of electrons through the De Broglie relation, the resolution of EM can be predicted.

$$\lambda = \frac{h}{mv} = \frac{h}{\sqrt{2mE_k}} \tag{6}$$

$$E_k = eV = \frac{1}{2}mv^2 \tag{7}$$

In the De Broglie relation, the wavelength λ is proportional to Planck's constant h and inversely proportional to the electron momentum, E_k is the kinetic energy of the electron multiplied by the electron charge e and the accelerating voltage V, and m and v are the mass and velocity of the electron, respectively. The wavelength and velocity of the electron can be controlled through the electron's accelerating voltage. Hence, the larger the accelerating voltage, the closer the electron comes to the speed of light, and the shorter its wavelength becomes.
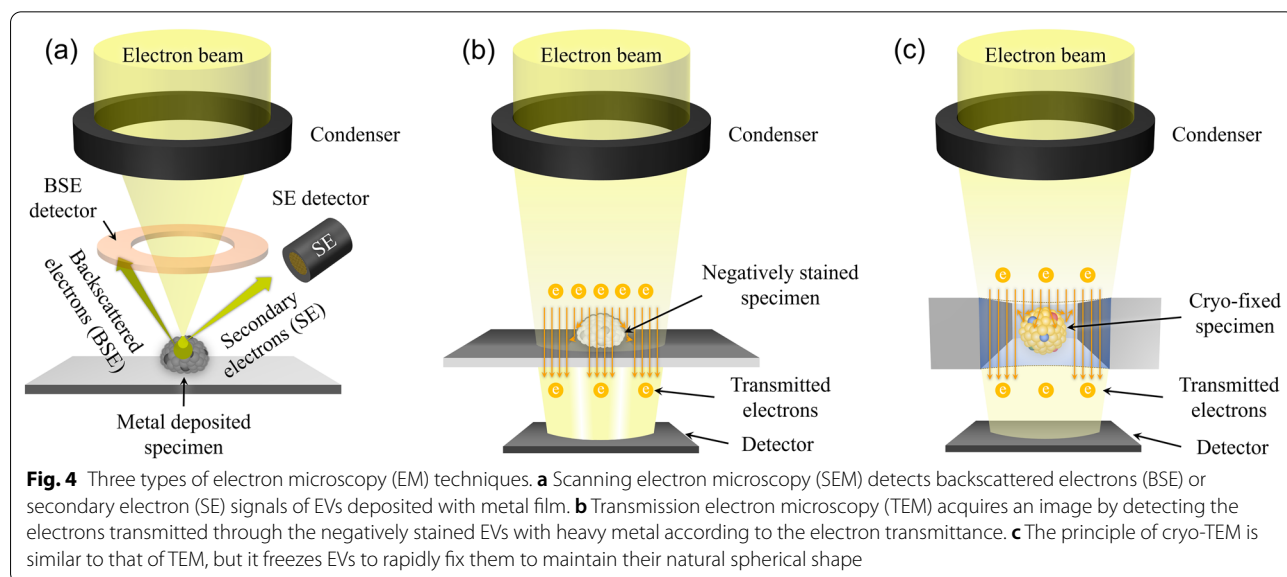
EM can theoretically have resolution of several picometers. However, in reality, it has resolution of about 1 nm due to imperfect electronic lenses and imaging environments. Nevertheless, it is possible to analyze the shape of EVs at a resolution that cannot be achieved with optical microscopy owing to the short wavelength of electrons [65, 66].

The methods using the received electron signal to determine the state of the sample are largely divided into scanning electron microscopy (SEM) and a transmission electron microscopy (TEM). SEM is a technique that detects backscattered electrons (BSE) or secondary electrons (SE) from a focused electron beam illuminating specimens and reconstructs them via data processing (Fig. 4a). To use SEM to observe EVs, which are nonconductive, they must be coated with a thin metal film to scatter the electrons [67]. In general, SEM is an efficient method to observe the appearance of EVs. however, the external shape of EVs is deformed while attaching the EVs to the surface, and it is difficult to distinguish between different particles. The metallic coating also makes it difficult to observe the inside of the phospholipid bilayer.

In contrast, TEM can observe the interior of EV at high resolution using a broad electron beam (Fig. 4b). To observe EVs by TEM, the exosomes fixed to the grid supporting the sample are negatively stained with a heavy metal. Depending on the amount of heavy metal coating, EVs can be distinguished in terms a bright region and in a dark peripheral region that does not transmit electrons. In TEM imaging, at the stage of attaching the sample to the grid, the dehydrated EVs do not maintain a complete spherical shape and look like a cup shape.

Dehydrated EVs pose a limitation in terms of morphology analysis, and cryo-TEM is used to observe their natural shape (Fig. 4c) [47]. Cryo-TEM is advantageous for the analysis of EVs in pure body fluid without dehydration, staining, or chemical fixation and is an excellent technique for observing the spherical shape of EVs in their natural state [1]. In cryo-TEM imaging, EVs inside small droplets are deposited on a grid and rapidly frozen (about -180 ℃) with ethane (cryogen) for observation. EVs inside the quick-frozen thin liquid film are in a native frozen-hydrated state and look like a spherical shape without deformation via the transmitted electronic signal [68]. The resolution of the cryo-TEM is approximately 2 nm, and it is possible to visualize the phospholipid bilayer, such that vesicles and other impurities can be distinguished by imaging [69–71].

The immuno-EM method, which negatively stains EVs with specific markers using an antibody bound to gold nanoparticles, enables conventional EM to observe not only morphology but also the biological phenotype. Gold particles do not transmit electrons and therefore appear as dark phases, such that the presence and location of protein markers can be identified. Using immuno-EM, Kim et al. reported that anti-programmed cell death protein ligand-1 (PD-L1) is expressed on the outer membrane of lung cancer cell-derived EVs [72]. In addition to observing a two-dimensional (2D) image of EVs, there is also a technique for volumetric observation of its three-dimensional (3D) structure. The 3D shape is analyzed without EV dehydration through serial sectioning block face scanning electron microscopy (SBEM) and a focused

Fig. 4 Three types of electron microscopy (EM) techniques. **a** Scanning electron microscopy (SEM) detects backscattered electrons (BSE) or secondary electron (SE) signals of EVs deposited with metal film. **b** Transmission electron microscopy (TEM) acquires an image by detecting the electrons transmitted through the negatively stained EVs with heavy metal according to the electron transmittance. **c** The principle of cryo-TEM is similar to that of TEM, but it freezes EVs to rapidly fix them to maintain their natural spherical shape

ion beam SEM (FIB-SEM), which cuts the EV-fixed block directly through an ultramicrotome or focused gallium ion beam at intervals of about 15 nm [70, 73, 74]. The physically cut EVs are volumetrically reconstructed into a 3D shape using a computer program, enabling sophisticated shape analysis of the inside and outside of the EV [75, 76].
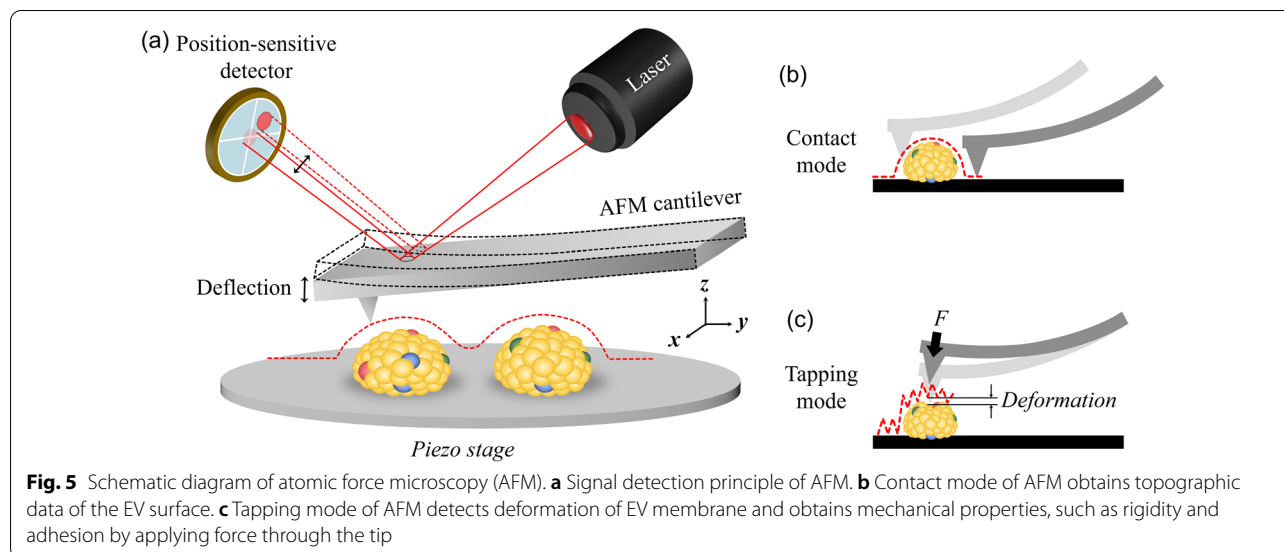
Atomic force microscopy (AFM)
AFM is a type of scanning probe microscopy. Among non-optical analysis methods, AFM is preferred for the analysis of non-conductive bioparticles, along with TEM (Fig. 5a). EVs immobilized by electrostatic interactions on the mica substrate disc are placed on a metal jig, and their external shape is scanned by a tip (Fig. 5b). The tapping mode uses a vibrating cantilever while scanning the sample to detect membrane deflection through the laser and photodiode and obtain 3D shape information and mechanical properties, such as stiffness, bending modulus, and adhesion (Fig. 5c) [77–80]. Debris or salts attached to the surface other than EVs act as noise in AFM imaging and require sufficient washing before analysis, and impurities that are not removed ($\sim$ 3 nm) can be distinguished from EVs by z-axis size-based thresholding [81].

The binding force between proteins can be analyzed using the force applied to the tip. Mechanical properties, such as the EV membrane or chemical bonding force through the sharp tip, can be measured, which is essential for understanding drug delivery and interactions between cells and particles by analyzing the deformation properties and mechanical stability of EVs [65, 82]. Sharma et al. confirmed that the deformation

of the EV membrane increased according to the force applied to the tip and made the central depression more evident. The physical properties of the immune-stained membrane protein are measured with an antibody bound to gold beads. The binding force of membrane proteins and their presence on the surface are analyzed through single antigen–antibody complex bond ruptures of CD63 [65].

Furthermore, using the force mapping mode of 3D-AFM, it is possible to analyze the nano-mechanical properties of EVs. Yurtsever et al. measured Young's modulus of metastatic tumor cells (143B) and non-metastatic cell-derived exosomes in the range of $\sim$ 50 to 350 MPa. Highly aggressive metastatic 143B cell-derived exosomes (about 192 MPa) have higher membrane stiffness than non-metastatic cell-derived exosomes (about 118 MPa) [82]. This difference in elasticity is attributed to the difference in membrane protein components of cell-derived exosomes according to metastasis, even in the same cell line, and protein analysis confirmed that more elastic fiber-associated proteins are expressed in exosomes. The composition of lipid components and membrane proteins is related to the membrane stiffness, which is consistent with the results of various reports [83–87].

Ridolfi et al. introduced a technique for discriminating nano-sized vesicles and non-vesicular objects attached to a substrate by electrostatic interaction based on AFM image data. The spherical particle diameter is predicted using the height of the vesicle deformed by attachment, the contact angle of the vesicle surface, and the surface-projected radius. The authors reported that EVs of different origins had very similar contact angles and it is

Fig. 5 Schematic diagram of atomic force microscopy (AFM). **a** Signal detection principle of AFM. **b** Contact mode of AFM obtains topographic data of the EV surface. **c** Tapping mode of AFM detects deformation of EV membrane and obtains mechanical properties, such as rigidity and adhesion by applying force through the tip

possible to classify EVs and impurities based on the contact angle value. Physical characteristic analysis cannot be more accurate than force spectroscopy (FS), but it is reported that some predictability is possible with imaging-based analysis [79]. Calò et al. calculated Young's modulus using FS for various nano-sized vesicles according to phospholipid and protein composition. They compared Young's modulus of the three types of vesicles: synthetic liposome, natural vesicle, and virus compressed a protein shell, suggesting that the presence of membrane proteins plays a role in enhancing membrane stiffness and imparting mechanical stability [88].

Resistive pulse sensing (RPS)

RPS detects electrical changes caused by non-conducting biomolecules in aqueous solutions passing through electrodes [7, 89, 90]. It has been widely applied to the characteristic study of single particles with a high precision and accuracy [91–93]. The structure of the RPS consists of two chambers and electrodes, divided on the basis of a porous plate. A current is generated by a potential difference on both sides of the pore, and resistance increases at that moment when the particle with low conductivity passes through the pore (Fig. 6a). The increase in resistance reduces the current signal, and the size of the particles passing through the pores and the zeta potential can be measured through the reduced current strength and duration time. Furthermore, the concentration of nanoparticles can be analyzed by measuring the number

of resistive pulses that the particles pass through the pore per unit time. In the cylindrical model, the relative change in the resistance when a spherical particle passes through a cylindrical pore is described as follows:

$$\frac{\Delta R}{R} \sim \frac{d^3}{D^2 L} \tag{8}$$

In the left term representing the relative resistance change, ΔR is the resistance change and R is the resistance of the medium filling the pore. d is the diameter of the particle and D and L denote the diameter and length of the pores, respectively [94]. Particles are moved by diffusion and pressure-driven fluxes, electrophoretic forces depending on the zeta potential of particles, and electroosmotic forces of the medium [94]. The actual resistance change depends on the properties of the particles passing through the pore, the degree to which it occupies the surrounding medium, and the geometric diversity of the pore (Fig. 6b) [91, 95, 96].

Tunable RPS (TRPS), an advanced RPS technology, improves the accuracy in measuring the size and concentration of nanoparticles, such as EVs, by controlling the pore size [90, 95]. For the accurate measurement of exosomes, variables such as the pore size and voltage are optimized, and agglomeration of particles is prevented through a surfactant, enabling the analysis of particles with ~37 nm diameter [92]. TRPS can distinguish polydisperse samples of various sizes at a higher resolution than various optical techniques capable of
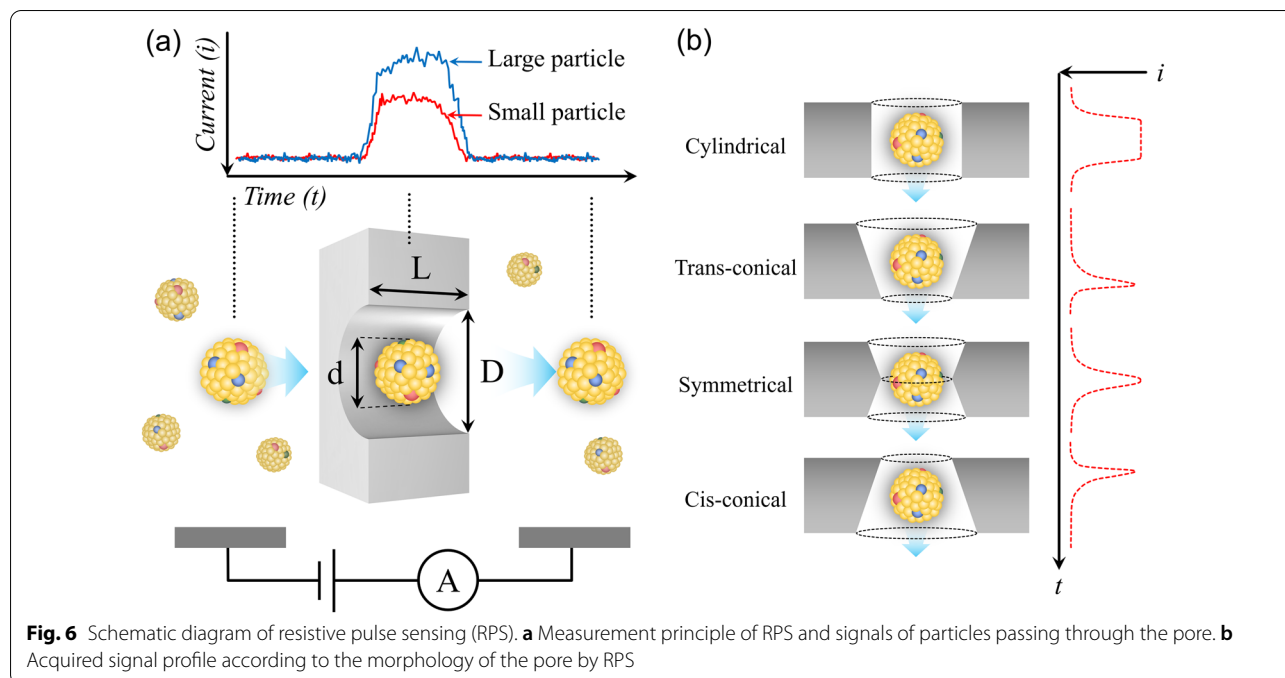
Fig. 6 Schematic diagram of resistive pulse sensing (RPS). **a** Measurement principle of RPS and signals of particles passing through the pore. **b** Acquired signal profile according to the morphology of the pore by RPS

Table 1 Comparison of single EV analysis techniques

Type	Optical techniques			Non-optical techniques					
	NTA	nFCM	TIRF & Dark-field	Electron microscopy			AFM	RPS
				SEM	TEM	Cryo-TEM		
Sample state	Suspension	Suspension	Immobilized, diffusion	Immobilized, dehydrated	Immobilized, dehydrated	Immobilized	Immobilized, dehydrated	Suspension
Detection type	Light scattering, fluorescence	Light scattering, fluorescence	Light scattering, fluorescence	Scattered electron	Transmitted electron	Transmitted electron	Light position	Electric current
Detection size	> 50 nm	> 50 nm	> 30–40 nm	> 1–2 nm	> 1–2 nm	> 1–2 nm	> 1 nm	> 40 nm
Size	○	○	✕	◎	◎	◎	◎	◎
Concentration	◎	◎	✕	✕	✕	✕	✕	◎
Shape	✕	✕	✕	◎	◎	◎	○	✕
Phenotype	◎	◎	◎	✕	○	○	✕	✕
Rigidity	✕	✕	✕	✕	✕	✕	◎	✕
Charge	○	✕	✕	✕	✕	✕	✕	◎

◎: nice technique; ○: good technique; ✕: none

quantitative analysis of numerous particles in aqueous solution. Compared with optical-based analysis techniques such as NTA, DLS, and nFCM, the size resolution of monomodal and multimodal samples of four sizes and the concentration measurement of each size are possible with very high accuracy [97].

Conclusion

EVs are in vivo nanocarriers that act as intercellular communication and tumor progression mediators. Since the first discovery, EVs are particularly noted for their potential for drug delivery and clinical diagnosis [2–5, 98]. EVs not only have various components, depending on the cell line, but also have heterogeneous characteristics in the EV population derived from the same cell line. They are intrinsically complex, considering the variety of purposes they serve. Therefore, it is necessary to distinguish these heterogeneous EVs and to reveal their roles.

The difficulties of optical measurement due to the diffraction limit of visible light and the analysis of bioparticles in a conventional EM have been solved through the technology advancements, and the analysis of single nanoparticles has become possible for more than a decade. Through the advancement of these technologies, the limitations of the ensemble analyses of EVs, such as the western blot, enzyme-linked immunosorbent assay, and polymerase chain reaction, have been solved. In the guidelines for minimal information for studies of extracellular vesicles (MISEV), it was suggested that in the study of single EVs, at least two or more single particle analyses, such as morphology and biological characteristics, must be performed. Hence, it is necessary to rigorously analyze EVs in various ways by reflecting the

diversity of rapidly advancing analysis technologies. Researchers must select the technologies suitable for the purpose of analysis (Table 1) [10]. In conclusion, single EV analysis of appropriate combinations is a gateway that must be crossed to understand physiological and pathological characteristics of EVs and study biomarkers for drug delivery and diagnosis in the EV research field.

Author contributions
YM surveyed previous works and wrote the manuscript. JP provided advice for the manuscript. Both authors read and approved the final manuscript.

Availability of data and materials
Not applicable.

Declarations

Author details
[1]Department of Mechanical Engineering, Pohang University of Science and Technology (POSTECH), Pohang, Gyeong-buk 37673, Republic of Korea. [2]School of Interdisciplinary Bioscience and Bioengineering, Pohang University of Science and Technology (POSTECH), Pohang, Gyeong-buk 37673, Republic of Korea.

References

1. Raposo G, Stoorvogel W (2013) Extracellular vesicles: exosomes, microvesicles, and friends. J Cell Biol 200(4):373–383. https://doi.org/10.1083/jcb.201211138
2. van Dommelen SM, Vader P, Lakhal S, Kooijmans SA, van Solinge WW, Wood MJ, Schiffelers RM (2012) Microvesicles and exosomes: opportunities for cell-derived membrane vesicles in drug delivery. J Control Release 161(2):635–644. https://doi.org/10.1016/j.jconrel.2011.11.021
3. Li XH, Zhang J, Li DF, Wu W, Xie ZW, Liu Q (2020) Physiological and pathological insights into exosomes in the brain. Zool Res 41(4):365–372. https://doi.org/10.24272/j.issn.2095-8137.2020.043
4. van Blitterswijk WJ, Emmelot P, Hilkmann HAM, Hilgers J, Feltkamp CA (1979) Rigid plasma-membrane-derived vesicles, enriched in tumour-associated surface antigens (MLr), occurring in the ascites fluid of a murine leukaemia (GRSL). Int J Cancer 23(1):62–70. https://doi.org/10.1002/ijc.2910230112
5. Friend C, Marovitz W, Henie G, Henie W, Tsuei D, Hirschhorn K, Holland JG, Cuttner J (1978) Observations on cell lines derived from a patient with Hodgkin's disease. Cancer Res 38(8):2581–2591
6. Piffoux M, Silva AKA, Wilhelm C, Gazeau F, Tareste D (2018) Modification of extracellular vesicles by fusion with liposomes for the design of personalized biogenic drug delivery systems. ACS Nano 12(7):6830–6842. https://doi.org/10.1021/acsnano.8b02053
7. Vogel R, Savage J, Muzard J, Camera GD, Vella G, Law A, Marchioni M, Mehn D, Geiss O, Peacock B, Aubert D, Calzolai L, Caputo F, Prina-Mello A (2021) Measuring particle concentration of multimodal synthetic reference materials and extracellular vesicles with orthogonal techniques: who is up to the challenge? J Extracell Vesicles 10(3):e12052. https://doi.org/10.1002/jev2.12052
8. Kang H, Kim J, Park J (2017) Methods to isolate extracellular vesicles for diagnosis. Micro Nano Syst Lett. https://doi.org/10.1186/s40486-017-0049-7
9. Doyle LM, Wang MZ (2019) Overview of extracellular vesicles, their origin, composition, purpose, and methods for exosome isolation and analysis. Cells. https://doi.org/10.3390/cells8070727
10. Thery C, Witwer KW, Aikawa E, Alcaraz MJ, Anderson JD, Andriantsitohaina R, Antoniou A, Arab T, Archer F, Atkin-Smith GK, Ayre DC, Bach JM, Bachurski D, Baharvand H, Balaj L, Baldacchino S, Bauer NN, Baxter AA, Bebawy M, Zuba-Surma EK (2018) Minimal information for studies of extracellular vesicles 2018 (MISEV2018): a position statement of the international society for extracellular vesicles and update of the MISEV2014 guidelines. J Extracell Vesicles 7(1):1535750. https://doi.org/10.1080/20013078.2018.1535750
11. Min L, Wang B, Bao H, Li X, Zhao L, Meng J, Wang S (2021) Advanced nanotechnologies for extracellular vesicle-based liquid biopsy. Adv Sci (Weinh) 8(20):e2102789. https://doi.org/10.1002/advs.202102789
12. Chiang CY, Chen C (2019) Toward characterizing extracellular vesicles at a single-particle level. J Biomed Sci 26(1):9. https://doi.org/10.1186/s12929-019-0502-4
13. Bagci C, Sever-Bahcekapili M, Belder N, Bennett APS, Erdener SE, Dalkara T (2022) Overview of extracellular vesicle characterization techniques and introduction to combined reflectance and fluorescence confocal

microscopy to distinguish extracellular vesicle subpopulations. Neurophotonics 9(2):021903. https://doi.org/10.1117/1.NPh.9.2.021903
14. Lipson A, Lipson SG, Lipson H (2010) Optical physics. Cambridge University Press, Cambridge. https://doi.org/10.1017/CBO9780511763120
15. Dragovic RA, Gardiner C, Brooks AS, Tannetta DS, Ferguson DJ, Hole P, Carr B, Redman CW, Harris AL, Dobson PJ, Harrison P, Sargent IL (2011) Sizing and phenotyping of cellular vesicles using nanoparticle tracking analysis. Nanomedicine 7(6):780–788. https://doi.org/10.1016/j.nano.2011.04.003
16. Sage D, Kirshner H, Pengo T, Stuurman N, Min J, Manley S, Unser M (2015) Quantitative evaluation of software packages for single-molecule localization microscopy. Nat Methods 12(8):717–724. https://doi.org/10.1038/nmeth.3442
17. Jimenez A, Friedl K, Leterrier C (2020) About samples, giving examples: optimized single molecule localization microscopy. Methods 174:100–114. https://doi.org/10.1016/j.ymeth.2019.05.008
18. Shen H, Tauzin LJ, Baiyasi R, Wang W, Moringo N, Shuang B, Landes CF (2017) Single particle tracking: from theory to biophysical applications. Chem Rev 117(11):7331–7376. https://doi.org/10.1021/acs.chemrev.6b00815
19. Deschout H, Cella Zanacchi F, Mlodzianoski M, Diaspro A, Bewersdorf J, Hess ST, Braeckmans K (2014) Precisely and accurately localizing single emitters in fluorescence microscopy. Nat Method 11(3):253–266. https://doi.org/10.1038/nmeth.2843
20. Stehr F (2021) Advancing quantitative DNA-mediated single-molecule fluorescence microscopy (Doctoral dissertation, lmu). https://doi.org/10.5282/edoc.29117
21. Rose KA, Molaei M, Boyle MJ, Lee D, Crocker JC, Composto RJ (2020) Particle tracking of nanoparticles in soft matter. J Appl Phys. https://doi.org/10.1063/5.0003322
22. Bian X, Kim C, Karniadakis GE (2016) 111 years of Brownian motion. Soft Matter 12(30):6331–6346. https://doi.org/10.1039/c6sm01153e
23. Kim A, Ng WB, Bernt W, Cho NJ (2019) Validation of size estimation of nanoparticle tracking analysis on polydisperse macromolecule assembly. Sci Rep 9(1):2639. https://doi.org/10.1038/s41598-019-38915-x
24. Hole P, Sillence K, Hannell C, Maguire CM, Roesslein M, Suarez G, Capracotta S, Magdolenova Z, Horev-Azaria L, Dybowska A, Cooke L, Haase A, Contal S, Mano S, Vennemann A, Sauvain JJ, Staunton KC, Anguissola S, Luch A, Wick P (2013) Interlaboratory comparison of size measurements on nanoparticles using nanoparticle tracking analysis (NTA). J Nanopart Res 15:2101. https://doi.org/10.1007/s11051-013-2101-8
25. El-Andaloussi S, Lee Y, Lakhal-Littleton S, Li J, Seow Y, Gardiner C, Alvarez-Erviti L, Sargent IL, Wood MJ (2012) Exosome-mediated delivery of siRNA in vitro and in vivo. Nat Protoc 7(12):2112–2126. https://doi.org/10.1038/nprot.2012.131
26. Carr B, Wright M (2013) Nanoparticle tracking analysis: a review of applications and usage 2010–2012. Nanosight
27. Weber A, Wehmeyer JC, Schmidt V, Lichtenberg A, Akhyari P (2019) Rapid fluorescence-based characterization of single extracellular vesicles in human blood with nanoparticle-tracking analysis. J Vis Exp. https://doi.org/10.3791/58731
28. Dehghani M, Gulvin SM, Flax J, Gaborski TR (2020) Systematic evaluation of PKH labelling on extracellular vesicle size by nanoparticle tracking analysis. Sci Rep 10(1):9533. https://doi.org/10.1038/s41598-020-66434-7
29. Szatanek R, Baj-Krzyworzeka M, Zimoch J, Lekka M, Siedlar M, Baran J (2017) The methods of choice for extracellular vesicles (EVs) characterization. Int J Mol Sci. https://doi.org/10.3390/ijms18061153
30. Dragovic RA, Collett GP, Hole P, Ferguson DJ, Redman CW, Sargent IL, Tannetta DS (2015) Isolation of syncytiotrophoblast microvesicles and exosomes and their characterisation by multicolour flow cytometry and fluorescence nanoparticle tracking analysis. Methods 87:64–74. https://doi.org/10.1016/j.ymeth.2015.03.028
31. Cho S, Yi J, Kwon Y, Kang H, Han C, Park J (2021) Multifluorescence single extracellular vesicle analysis by time-sequential illumination and tracking. ACS Nano. https://doi.org/10.1021/acsnano.1c02556
32. Melling GE, Conlon R, Pantazi P, Dellar ER, Samuel P, Baena-Lopez LA, Simpson JC, Carter DRF (2022) Confocal microscopy analysis reveals that only a small proportion of extracellular vesicles are successfully labelled with commonly utilised staining methods. Sci Rep 12(1):262. https://doi.org/10.1038/s41598-021-04225-4

33. Simonsen JB (2019) Pitfalls associated with lipophilic fluorophore staining of extracellular vesicles for uptake studies. J Extracell Vesicles 8(1):1582237. https://doi.org/10.1080/20013078.2019.1582237

34. Kerker M, Chew H, McNulty PJ, Kratohvil JP, Cooke DD, Sculley M, Lee MP (1979) Light scattering and fluorescence by small particles having internal structure. J Histochem Cytochem 27(1):250–263. https://doi.org/10.1177/27.1.438501

35. Tian Y, Ma L, Gong M, Su G, Zhu S, Zhang W, Wang S, Li Z, Chen C, Li L, Wu L, Yan X (2018) Protein profiling and sizing of extracellular vesicles from colorectal cancer patients via flow cytometry. ACS Nano 12(1):671–680. https://doi.org/10.1021/acsnano.7b07782

36. Nolte-'t Hoen EN, van der Vlist EJ, Aalberts M, Mertens HC, Bosch BJ, Bartelink W, Mastrobattista E, van Gaal EV, Stoorvogel W, Arkesteijn GJ, Wauben MH (2012) Quantitative and qualitative flow cytometric analysis of nanosized cell-derived membrane vesicles. Nanomedicine 8(5):712–720. https://doi.org/10.1016/j.nano.2011.09.006

37. Ma L, Zhu S, Tian Y, Zhang W, Wang S, Chen C, Wu L, Yan X (2016) Label-free analysis of single viruses with a resolution comparable to that of electron microscopy and the throughput of flow cytometry. Angew Chem Int Ed Engl 55(35):10239–10243. https://doi.org/10.1002/anie.201603007

38. van der Vlist EJ, Nolte-'t Hoen EN, Stoorvogel W, Arkesteijn GJ, Wauben MH (2012) Fluorescent labeling of nano-sized vesicles released by cells and subsequent quantitative and qualitative analysis by high-resolution flow cytometry. Nat Protoc 7(7):1311–1326. https://doi.org/10.1038/nprot.2012.065

39. Zhu S, Ma L, Wang S, Chen C, Zhang W, Yang L, Hang W, Nolan JP, Wu L, Yan X (2014) Light-scattering detection below the level of single fluorescent molecules for high-resolution characterization of functional nanoparticles. ACS Nano 8(10):10998–11006. https://doi.org/10.1021/nn505162u

40. Shapiro HM (2005) Practical flow cytometry. Wiley, Oxford. https://doi.org/10.1002/0471722731

41. Steen HB (2004) Flow cytometer for measurement of the light scattering of viral and other submicroscopic particles. Cytometry 57A(2):94–99. https://doi.org/10.1002/cyto.a.10115

42. Libregts S, Arkesteijn GJA, Nemeth A, Nolte-'t Hoen ENM, Wauben MHM (2018) Flow cytometric analysis of extracellular vesicle subsets in plasma: impact of swarm by particles of non-interest. J Thromb Haemost 16(7):1423–1436. https://doi.org/10.1111/jth.14154

43. Morales-Kastresana A, Telford B, Musich TA, McKinnon K, Clayborne C, Braig Z, Rosner A, Demberg T, Watson DC, Karpova TS, Freeman GJ, DeKruyff RH, Pavlakis GN, Terabe M, Robert-Guroff M, Berzofsky JA, Jones JC (2017) Labeling extracellular vesicles for nanoscale flow cytometry. Sci Rep 7(1):1878. https://doi.org/10.1038/s41598-017-01731-2

44. Groot Kormelink T, Arkesteijn GJ, Nauwelaers FA, van den Engh G, Nolte-'t Hoen EN, Wauben MH (2016) Prerequisites for the analysis and sorting of extracellular vesicle subpopulations by high-resolution flow cytometry. Cytometry A 89(2):135–147. https://doi.org/10.1002/cyto.a.22644

45. Arraud N, Gounou C, Linares R, Brisson AR (2015) A simple flow cytometry method improves the detection of phosphatidylserine-exposing extracellular vesicles. J Thromb Haemost 13(2):237–247. https://doi.org/10.1111/jth.12767

46. Ter-Ovanesyan D, Kowal EJK, Regev A, Church GM, Cocucci E (2017) Imaging of isolated extracellular vesicles using fluorescence microscopy. Methods Mol Biol 1660:233–241. https://doi.org/10.1007/978-1-4939-7253-1_19

47. Silva AM, Lazaro-Ibanez E, Gunnarsson A, Dhande A, Daaboul G, Peacock B, Osteikoetxea X, Salmond N, Friis KP, Shatnyeva O, Dekker N (2021) Quantification of protein cargo loading into engineered extracellular vesicles at single-vesicle and single-molecule resolution. J Extracell Vesicles 10(10):e12130. https://doi.org/10.1002/jev2.12130

48. Han C, Kang H, Yi J, Kang M, Lee H, Kwon Y, Jung J, Lee J, Park J (2021) Single-vesicle imaging and co-localization analysis for tetraspanin profiling of individual extracellular vesicles. J Extracell Vesicles 10(3):e12047. https://doi.org/10.1002/jev2.12047

49. Lee J, Kwon Y, Jung J, Shin H, Park J (2021) Immunostaining extracellular vesicles based on an aqueous two-phase system: for analysis of tetraspanins. ACS Appl Bio Mater 4(4):3294–3303. https://doi.org/10.1021/acsabm.0c01625

50. Olsson T, Zhdanov VP, Höök F (2015) Total internal reflection fluorescence microscopy for determination of size of individual immobilized vesicles: theory and experiment. J Appl Phys 118(6):064702. https://doi.org/10.1063/1.4928083

51. Shen L-M, Quan L, Liu J (2018) Tracking exosomes in vitro and in vivo to elucidate their physiological functions: implications for diagnostic and therapeutic nanocarriers. ACS Appl Nano Mater 1(6):2438–2448. https://doi.org/10.1021/acsanm.8b00601

52. Ewers H, Smith AE, Sbalzarini IF, Lilie H, Koumoutsakos P, Helenius A (2005) Single-particle tracking of murine polyoma virus-like particles on live cells and artificial membranes. Proc Natl Acad Sci U S A 102(42):15110–15115. https://doi.org/10.1073/pnas.0504407102

53. Gul B, Ashraf S, Khan S, Nisar H, Ahmad I (2021) Cell refractive index: models, insights, applications and future perspectives. Photodiagnosis Photodyn Ther 33:102096. https://doi.org/10.1016/j.pdpdt.2020.102096

54. Liu PY, Chin LK, Ser W, Chen HF, Hsieh CM, Lee CH, Sung KB, Ayi TC, Yap PH, Liedberg B, Wang K, Bourouina T, Leprince-Wang Y (2016) Cell refractive index for cell biology and disease diagnosis: past, present and future. Lab Chip 16(4):634–644. https://doi.org/10.1039/c5lc01445j

55. Hoshino D, Kirkbride KC, Costello K, Clark ES, Sinha S, Grega-Larson N, Tyska MJ, Weaver AM (2013) Exosome secretion is enhanced by invadopodia and drives invasive behavior. Cell Rep 5(5):1159–1168. https://doi.org/10.1016/j.celrep.2013.10.050

56. He D, Wang H, Ho SL, Chan HN, Hai L, He X, Wang K, Li HW (2019) Total internal reflection-based single-vesicle in situ quantitative and stoichiometric analysis of tumor-derived exosomal microRNAs for diagnosis and treatment monitoring. Theranostics 9(15):4494–4507. https://doi.org/10.7150/thno.33683

57. Jiang Y, Andronico LA, Jung SR, Chen H, Fujimoto B, Vojtech L, Chiu DT (2021) High-throughput counting and superresolution mapping of tetraspanins on exosomes using a single-molecule sensitive flow technique and transistor-like semiconducting polymer dots. Angew Chem Int Ed Engl 60(24):13470–13475. https://doi.org/10.1002/anie.202103282

58. Raschke G, Brogl S, Susha AS, Rogach AL, Klar TA, Feldmann J, Fieres B, Petkov N, Bein T, Nichtl A, Kürzinger K (2004) Gold nanoshells improve single nanoparticle molecular sensors. Nano Lett 4(10):1853–1857. https://doi.org/10.1021/nl049038q

59. Hartland GV (2011) Optical studies of dynamics in noble metal nanostructures. Chem Rev 111(6):3858–3887. https://doi.org/10.1021/cr1002547

60. Schultz S, Smith DR, Mock JJ, Schultz DA (2000) Single-target molecule detection with nonbleaching multicolor optical immunolabels. Proc Natl Acad Sci 97(3):996–1001. https://doi.org/10.1073/pnas.97.3.996

61. Li T, Wu X, Liu F, Li N (2017) Analytical methods based on the light-scattering of plasmonic nanoparticles at the single particle level with dark-field microscopy imaging. Analyst 142(2):248–256. https://doi.org/10.1039/c6an02384c

62. Ekiz-Kanik F, Sevenler DD, Ünlü NL, Chiari M, Ünlü MS (2017) Surface chemistry and morphology in single particle optical imaging. Nanophotonics 6(4):713–730. https://doi.org/10.1515/nanoph-2016-0184

63. Enoki S, Iino R, Morone N, Kaihatsu K, Sakakihara S, Kato N, Noji H (2012) Label-free single-particle imaging of the influenza virus by objective-type total internal reflection dark-field microscopy. PLoS ONE 7(11):e49208. https://doi.org/10.1371/journal.pone.0049208

64. Akagi T, Kato K, Hanamura N, Kobayashi M, Ichiki T (2014) Evaluation of desialylation effect on zeta potential of extracellular vesicles secreted from human prostate cancer cells by on-chip microcapillary electrophoresis. Jpn J Appl Phys. https://doi.org/10.7567/jjap.53.06jl01

65. Sharma S, Rasool HI, Palanisamy V, Mathisen C, Schmidt M, Wong DT, Gimzewski JK (2010) Structural-mechanical characterization of nanoparticle exosomes in human saliva, using correlative AFM, FESEM, and force spectroscopy. ACS Nano 4(4):1921–1926. https://doi.org/10.1021/nn901824n

66. Noble JM, Roberts LM, Vidavsky N, Chiou AE, Fischbach C, Paszek MJ, Estroff LA, Kourkoutis LF (2020) Direct comparison of optical and electron microscopy methods for structural characterization of extracellular vesicles. J Struct Biol 210(1):107474. https://doi.org/10.1016/j.jsb.2020.107474

67. Rupert DLM, Claudio V, Lasser C, Bally M (2017) Methods for the physical characterization and quantification of extracellular vesicles in biological samples. Biochim Biophys Acta Gen Subj 1861(1 Pt A):3164–3179. https://doi.org/10.1016/j.bbagen.2016.07.028

68. Arraud N, Linares R, Tan S, Gounou C, Pasquet JM, Mornet S, Brisson AR (2014) Extracellular vesicles from blood plasma: determination of their morphology, size, phenotype and concentration. J Thromb Haemost 12(5):614–627. https://doi.org/10.1111/jth.12554

69. Romero-Brey I, Merz A, Chiramel A, Lee JY, Chlanda P, Haselman U, Santarella-Mellwig R, Habermann A, Hoppe S, Kallis S, Walther P, Antony C, Krijnse-Locker J, Bartenschlager R (2012) Three-dimensional architecture and biogenesis of membrane structures associated with hepatitis C virus replication. PLoS Pathog 8(12):e1003056. https://doi.org/10.1371/journal.ppat.1003056

70. Choi H, Mun JY (2017) Structural analysis of exosomes using different types of electron microscopy. Appl Microsc 47(3):171–175. https://doi.org/10.9729/am.2017.47.3.171

71. Emelyanov A, Shtam T, Kamyshinsky R, Garaeva L, Verlov N, Miliukhina I, Kudrevatykh A, Gavrilov G, Zabrodskaya Y, Pchelina S, Konevega A (2020) Cryo-electron microscopy of extracellular vesicles from cerebrospinal fluid. PLoS ONE 15(1):e0227949. https://doi.org/10.1371/journal.pone.0227949

72. Kim DH, Kim H, Choi YJ, Kim SY, Lee JE, Sung KJ, Sung YH, Pack CG, Jung MK, Han B, Kim K, Kim WS, Nam SJ, Choi CM, Yun M, Lee JC, Rho JK (2019) Exosomal PD-L1 promotes tumor growth through immune escape in non-small cell lung cancer. Exp Mol Med 51(8):1–13. https://doi.org/10.1038/s12276-019-0295-2

73. Baena V, Schalek RL, Lichtman JW, Terasaki M (2019) Serial-section electron microscopy using automated tape-collecting ultramicrotome (ATUM). Methods Cell Biol 152:41–67. https://doi.org/10.1016/bs.mcb.2019.04.004

74. Cretoiu D, Gherghiceanu M, Hummel E, Zimmermann H, Simionescu O, Popescu LM (2015) FIB-SEM tomography of human skin telocytes and their extracellular vesicles. J Cell Mol Med 19(4):714–722. https://doi.org/10.1111/jcmm.12578

75. Peddie CJ, Collinson LM (2014) Exploring the third dimension: volume electron microscopy comes of age. Micron 61:9–19. https://doi.org/10.1016/j.micron.2014.01.009

76. Briggman KL, Bock DD (2012) Volume electron microscopy for neuronal circuit reconstruction. Curr Opin Neurobiol 22(1):154–161. https://doi.org/10.1016/j.conb.2011.10.022

77. Li MI, Xu X, Xi N, Wang W, Xing X, Liu L (2021) Multiparametric atomic force microscopy imaging of single native exosomes. Acta Biochim Biophys Sin (Shanghai) 53(3):385–388. https://doi.org/10.1093/abbs/gmaa172

78. Vorselen D, Piontek MC, Roos WH, Wuite GJL (2020) Mechanical characterization of liposomes and extracellular vesicles, a protocol. Front Mol Biosci 7:139. https://doi.org/10.3389/fmolb.2020.00139

79. Ridolfi A, Brucale M, Montis C, Caselli L, Paolini L, Borup A, Boysen AT, Loria F, van Herwijnen MJC, Kleinjan M, Nejsum P, Zarovni N, Wauben MHM, Berti D, Bergese P, Valle F (2020) AFM-based high-throughput nanomechanical screening of single extracellular vesicles. Anal Chem 92(15):10274–10282. https://doi.org/10.1021/acs.analchem.9b05716

80. Yokota S, Kuramochi H, Okubo K, Iwaya A, Tsuchiya S, Ichiki T (2019) Extracellular vesicles nanoarray technology: Immobilization of individual extracellular vesicles on nanopatterned polyethylene glycol-lipid conjugate brushes. PLoS ONE 14(10):e0224091. https://doi.org/10.1371/journal.pone.0224091

81. Bagrov DV, Senkovenko AM, Nikishin II, Skryabin GO, Kopnin PB, Tchevkina EM (2021) Application of AFM, TEM, and NTA for characterization of exosomes produced by placenta-derived mesenchymal cells. J Phys Conf Ser 1942(1):012013. https://doi.org/10.1088/1742-6596/1942/1/012013

82. Yurtsever A, Yoshida T, Badami Behjat A, Araki Y, Hanayama R, Fukuma T (2021) Structural and mechanical characteristics of exosomes from osteosarcoma cells explored by 3D-atomic force microscopy. Nanoscale 13(13):6661–6677. https://doi.org/10.1039/d0nr09178b

83. Rawicz W, Olbrich K, McIntosh T, Needham D, Evans E (2000) Effect of chain length and unsaturation on elasticity of lipid bilayers. Biophys J 79(1):328–339. https://doi.org/10.1016/s0006-3495(00)76295-3

84. Dimova R (2014) Recent developments in the field of bending rigidity measurements on membranes. Adv Colloid Interface Sci 208:225–234. https://doi.org/10.1016/j.cis.2014.03.003

85. Sorkin R, Huisjes R, Boskovic F, Vorselen D, Pignatelli S, Ofir-Birin Y, Freitas Leal JK, Schiller J, Mullick D, Roos WH, Bosman G, Regev-Rudzki N,

Schiffelers RM, Wuite GJL (2018) Nanomechanics of extracellular vesicles reveals vesiculation pathways. Small 14(39):e1801650. https://doi.org/10.1002/smll.201801650

86. LeClaire M, Gimzewski J, Sharma S (2020) A review of the biomechanical properties of single extracellular vesicles. Nano Sel 2(1):1–15. https://doi.org/10.1002/nano.202000129

87. Morshed A, Karawdeniya BI, Bandara Y, Kim MJ, Dutta P (2020) Mechanical characterization of vesicles and cells: a review. Electrophoresis 41(7–8):449–470. https://doi.org/10.1002/elps.201900362

88. Calo A, Reguera D, Oncins G, Persuy MA, Sanz G, Lobasso S, Corcelli A, Pajot-Augy E, Gomila G (2014) Force measurements on natural membrane nanovesicles reveal a composition-independent, high Young's modulus. Nanoscale 6(4):2275–2285. https://doi.org/10.1039/c3nr05107b

89. Lane RE, Korbie D, Anderson W, Vaidyanathan R, Trau M (2015) Analysis of exosome purification methods using a model liposome system and tunable-resistive pulse sensing. Sci Rep 5:7639. https://doi.org/10.1038/srep07639

90. Buzas EI, Gardiner C, Lee C, Smith ZJ (2017) Single particle analysis: methods for detection of platelet extracellular vesicles in suspension (excluding flow cytometry). Platelets 28(3):249–255. https://doi.org/10.1080/09537104.2016.1260704

91. Blundell ELCJ, Mayne LJ, Billinge ER, Platt M (2015) Emergence of tunable resistive pulse sensing as a biosensor. Anal Methods 7(17):7055–7066. https://doi.org/10.1039/c4ay03023k

92. Anderson W, Lane R, Korbie D, Trau M (2015) Observations of tunable resistive pulse sensing for exosome analysis: improving system sensitivity and stability. Langmuir 31(23):6577–6587. https://doi.org/10.1021/acs.langmuir.5b01402

93. Maas SL, Broekman ML, de Vrij J (2017) Tunable resistive pulse sensing for the characterization of extracellular vesicles. Methods mol biol (Clifton, N.J.) 1545:21–33. https://doi.org/10.1007/978-1-4939-6728-5_2

94. Yang L, Yamamoto T (2016) Quantification of virus particles using nanopore-based resistive-pulse sensing techniques. Front Microbiol 7:1500. https://doi.org/10.3389/fmicb.2016.01500

95. Vogel R, Willmott G, Kozak D, Roberts GS, Anderson W, Groenewegen L, Glossop B, Barnett A, Turner A, Trau M (2011) Quantitative sizing of nano/microparticles with a tunable elastomeric pore sensor. Anal Chem 83(9):3499–3506. https://doi.org/10.1021/ac200195n

96. Liao C, Antaw F, Wuethrich A, Anderson W, Trau M (2020) Configurable miniaturized 3D pores for robust single-nanoparticle analysis. Small Struct. https://doi.org/10.1002/sstr.202000011

97. Arab T, Mallick ER, Huang Y, Dong L, Liao Z, Zhao Z, Gololobova O, Smith B, Haughey NJ, Pienta KJ, Slusher BS, Tarwater PM, Tosar JP, Zivkovic AM, Vreeland WN, Paulaitis ME, Witwer KW (2021) Characterization of extracellular vesicles and synthetic nanoparticles with four orthogonal single-particle analysis platforms. J Extracell Vesicles 10(6):e12079. https://doi.org/10.1002/jev2.12079

98. Ciardiello C, Cavallini L, Spinelli C, Yang J, Reis-Sobreiro M, de Candia P, Minciacchi VR, Di Vizio D (2016) Focus on extracellular vesicles: new frontiers in cell-to-cell communication in cancer. Int J Mol Sci 17(2):175. https://doi.org/10.3390/ijms17020175

Publisher's Note